Theoretical Investigation of Photomagnetic Properties of Oxo-Verdazyl Substituted Pyrenes.

ARTICLE *in* THE JOURNAL OF PHYSICAL CHEMISTRY A · APRIL 2013

Impact Factor: 2.69 · DOI: 10.1021/jp402756j · Source: PubMed

6 AUTHORS, INCLUDING:

Tumpa Sadhukhan
Indian Institute of Technology Bombay
5 PUBLICATIONS **6** CITATIONS
SEE PROFILE

Arun Pal
IIT Kharagpur
9 PUBLICATIONS **45** CITATIONS
SEE PROFILE

Iqbal Latif
Indian Institute of Technology Bombay
12 PUBLICATIONS **83** CITATIONS
SEE PROFILE

Sambhu N Datta
Indian Institute of Technology Bombay
128 PUBLICATIONS **930** CITATIONS
SEE PROFILE

THE JOURNAL OF PHYSICAL CHEMISTRY A

Article

pubs.acs.org/JPCA

Theoretical Investigation of Photomagnetic Properties of Oxoverdazyl-Substituted Pyrenes

Tumpa Sadhukhan, Shekhar Hansda, Arun K. Pal, Gurram V. Venkatakrishna, Iqbal A. Latif, and Sambhu N. Datta*

Department of Chemistry, Indian Institute of Technology Bombay, Powai, Mumbai 400 076, India

Supporting Information

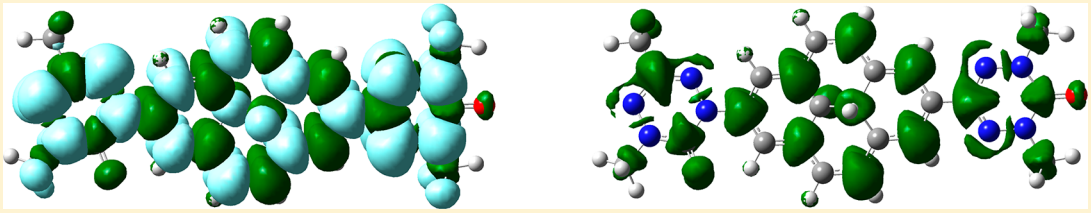

ABSTRACT: We have investigated the ground state spin of 10 pairs of possible photochromic diradical isomers by quantum chemical methods. Dihydrogen pyrenes and dinitrile pyrenes have been chosen as spacers with radical centers attached at (1,7) and (1,8) locations. Oxoverdazyl has served as a radical center, and both C and N linkages have been investigated. Triplet molecular geometries have been optimized at the UB3LYP/6-311G(d,p) level. Single-point calculations on triplet and broken symmetry states have been performed using the 6-311++G(d,p) basis set. Careful designs have led to the prediction of strongly coupled dihydropyrene (DHP) isomers, and the cyclophenadiene (CPD) isomers have always been found as weakly coupled. The effect of the functional M06-2X has been investigated. Calculated TDDFT spectra have been sufficient to guarantee photochromism of the designed diradicals. It has been estimated that compounds of diradicals with large coupling constants in the DHP form would show a pronounced change in molar susceptibility on photoconversion. This has led us to identify two molecules that can serve as a photomagnetic switch at room temperature.

INTRODUCTION

The area of photomagnetism in molecules has been becoming increasingly more important in the field of electronics. Most of the presently known photomagnets are based on metal ions;[1] however, to get a greater flexibility and lighter materials, researchers are moving toward photomagnets of organic origin. In this connection, photochromic molecules such as azobenzenes, stilbenes, pyrenes, etc. play an important role. These materials are used in building optical storage devices.[2] On irradiadion with specific wavelengths of light, the photochromic materials change their geometrical and physical properties, which becomes important for photoswitching. If these molecules are used as a coupler between two magnetic centers, then the magnetic character of the resulting species can change on irradiation.[3] Such materials can serve as photomagnetic switches, especially when a spin crossover accompanies the conversion.

A number of nitronyl nitroxide diradicals have been synthesized with perfluorocyclopentene, and these have very small magnetic exchange coupling constants (J).[3a,4] However, Ciofini et al.,[5] Datta et al.,[6] and Shil and Misra[7] calculated J values using theoretical methods on organic molecules and predicted that photomagnetic systems can have large J values. It is generally estimated that photoisomerization leads to a change from a small coupling constant to a large one and vice versa while J retains its sign. This gives rise to a change from paramagnetism to diamagnetism when J is negative and weak to strong paramagnetism when J is positive, and the reverse, for a macroscopically large ensemble of these compounds. Scheme 1 provides a simple illustration of photochromism in organic diradicals, following a recent CASSCF/CASPT2 investigation on the CPD−DHP interconversion by Robb et al.[8] A spin crossover may be witnessed in rare cases.[6c] In 2009, Ciofini et al. were able to synthesize their proposed systems for excited state paramagnetism and generated experimental evidence for their theoretical observations.[9] These facts encourage the search for organic molecules that can exhibit a pronounced change of magnetic character on photoconversion and thereby can be useful for molecular electronics.

In this work, we have used pyrenes as photochromic spacers. Cyclophenadiene (CPD) and dihydropyrene (DHP)—the dihydrogen and the dinitrile derivatives—are examined in this work. On the absorption of UV radiation or heat, CPD converts to DHP, and by absorption in the visible region, DHP converts to CPD (Figure 1),[10] but CPD is thermodynamically less stable,[10d] so the equilibrium of conversion is more toward DHP. However, 15,16-dinitrile-CPD is relatively stable: Mitchell et. al[11] showed

Special Issue: Structure and Dynamics: ESDMC, IACS-2013

Received: March 20, 2013
Revised: April 23, 2013
Published: April 24, 2013

Scheme 1. Illustration of Photochromism in Organic Diradicals[a]

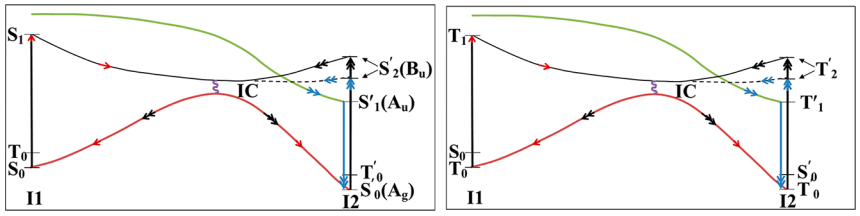

[a]I1 and I2 are isomers 1 and 2. The symmetry classification for singlet states is valid for DHP (I2). Two possible energy levels are shown for S'_2 ($J < 0$) and T'_2 ($J > 0$), with different consequences such as $S'_2 \rightarrow S'_1 \rightarrow S'_0$ and $S'_2 \rightarrow$ (IC) $\rightarrow S_0$. The possibility of spin crossover is not shown here. This general scheme has been prepared following Robb et al., ref 8.

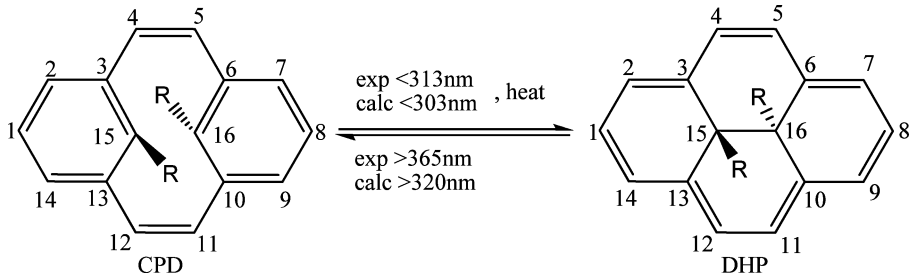

Figure 1. Interconversion of CPD and DHP by irradiation of specific wavelength of light. (Numbering has been taken from ref 12, and experimental data are from ref 13.) Similar diagrams have been used in refs 6a–c.

that 15,16-dinitrile-CPD derivatives can have a very long half-life (up to 30 years at 20 °C).

Williams et al.[12] carried out an extensive theoretical study of the energy barrier involved with different disubstituent derivatives. They found that the −CN groups are well placed to effectively conjugate with the π-systems on the two phenyl rings in the CPD form. This is why the dinitrile CPD derivatives are relatively more stable. The enthalpy of activation is larger (about 25 kcal mol^{-1}) for the dinitrile derivative, which enables the barrier to restrict thermal conversion. This is illustrated in scheme 2. The result is an increase in the lifetime of the dinitrile CPD and enhanced photochromism.

Oxoverdazyl (o-VER), has well-known magnetic properties.[14] It can be substituted at a carbon atom (C-terminal) as well as at a nitrogen atom (N-terminal), as shown in Figure 2. From

Scheme 2. Schematic Representation of the Potential Barrier for Conversion from Disubstituted CPD Derivative to DHP Derivative[a]

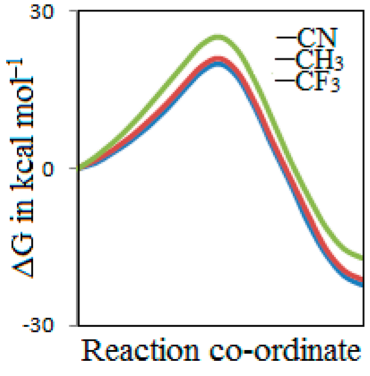

[a]This scheme has been prepared from the calculated data of Williams et al. (ref 12). Energy is in relative scale.

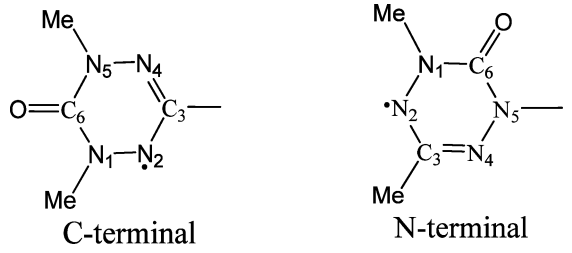

Figure 2. Oxoverdazyl moieties: (a) C4-terminal, (b) N6-terminal.

hyperfine coupling constants of the various atoms, Neugebauer et al.[15a] concluded that the spin is mainly distributed on atoms 2–4. Plater et al.[15b] showed that the species is sufficiently stable in crystal and is a $S = 1/2$ paramagnet. It is also generally known as a strong radical center.

The choice of oxoverdazyl has given rise to three combinations of photochromic diradical pairs that are based on two pairs of spacers (CPD and DHP forms, unsubstituted and dinitrile derivatives). These are illustrated in Figure 3. For the first and third combinations, i and iii, we have chosen radical centers with (1,8) and (1,7) substitutions on the pyrene ring. For the mixed combination, ii, only (1,8) substitutions have been chosen. Thus, 10 pairs of oxoverdazyl diradicals have been investigated:

(1,8)-dioxoVER(C)−15,16-dihydrogen CPD/DHP [**1a**, **1b**],
(1,8)-dioxoVER(C)−15,16-dinitrile CPD/DHP [**2a**, **2b**],
1-oxoVER(N)-8-oxoVER(C)−15,16-dihydrogen CPD/DHP [**3a**, **3b**],
1-oxoVER(N)-8-oxoVER(C)−15,16-dinitrile CPD/DHP [**4a**, **4b**],
(1,8)-dioxoVER(N)−15,16-dihydrogen CPD/DHP [**5a**, **5b**],
(1,8)-dioxoVER(N)−15,16-dinitrile CPD/DHP [**6a**, **6b**],

dx.doi.org/10.1021/jp402756j | J. Phys. Chem. A 2013, 117, 8609–8622

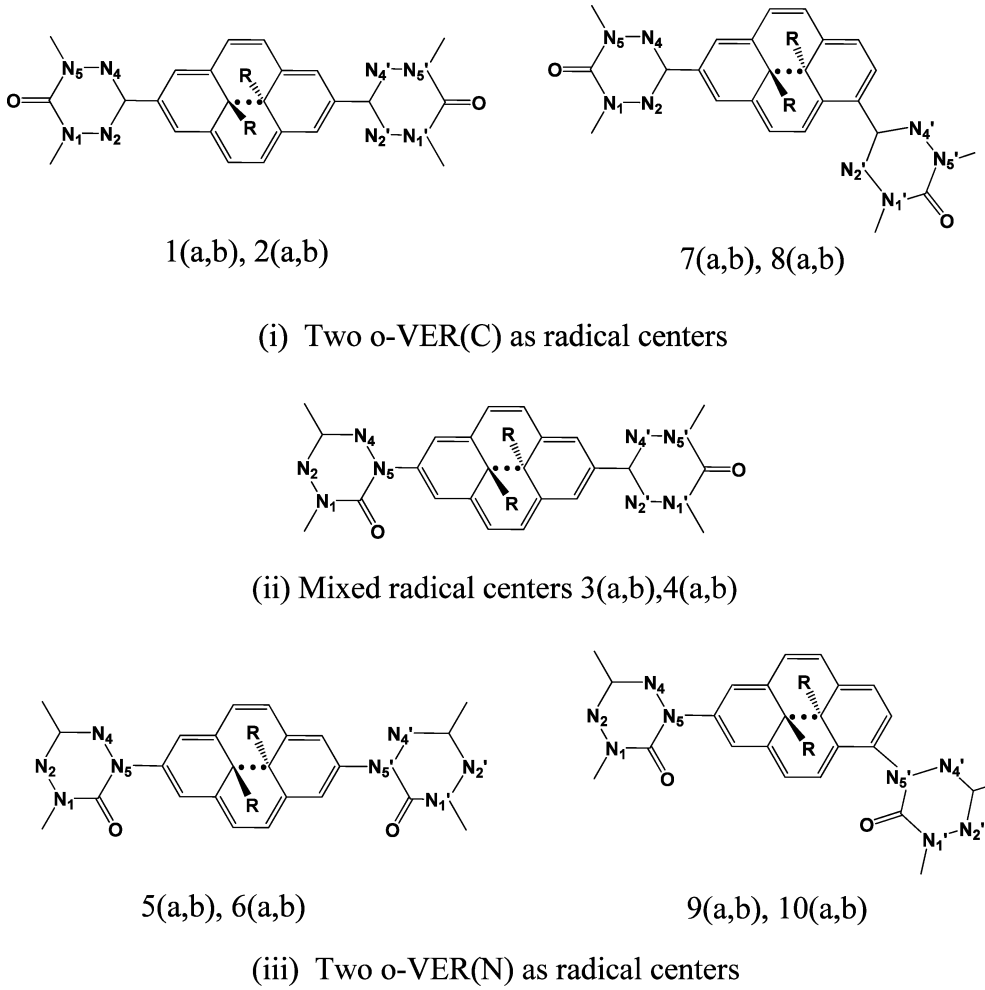

Figure 3. Diagrams showing different combinations of o-VER with spacer pyrene that stands for CPD and DHP with R as H and CN.

(1,7)-dioxoVER(C)−15,16-dihydrogen CPD/DHP [**7a**, **7b**],
(1,7)-dioxoVER(C)−15,16-dinitrile CPD/DHP [**8a**, **8b**],
(1,7)-dioxoVER(N)−15,16-dihydrogen CPD/DHP [**9a**, **9b**], and
(1,7)-dioxoVER(N)−15,16-dinitrile CPD/DHP [**10a**, **10b**].

In this work, our objectives have been 3-fold: First, we have quantum chemically evaluated the magnetic exchange coupling constants for the 10 pairs of diradicals. We show that in some cases, the diradicals are ferromagnetically coupled, whereas in other cases, they have singlet ground states. The nature of the ground states always agrees with the spin alternation rule[16] and the nondisjoint SOMO effect.[17a] As our second aim, we have estimated the absorption frequencies and oscillator strengths for transitions to the low-lying excited states and found that the transitions are sufficiently energetic and intense to ensure photochromic activity. Finally, we have investigated the change in paramagnetism that may be observed due to the interconversion of the diradical isomers in solvent, matrix, or solid state.

METHODOLOGY

The Heisenberg effective spin Hamiltonian is generally used to express the interaction of two spins S_1 and S_2 as

$$H = -2JS_1 \cdot S_2 \quad (1)$$

Here, J is the magnetic exchange coupling constant. A positive coupling constant holds for an intramolecular ferromagnetic interaction and triplet ground state, whereas a negative J is an indicator of the antiferromagnetic nature of intramolecular magnetic coupling that leads to a singlet ground state. For a biradical, the J value can be obtained from the spin-polarized solutions of triplet ($S = 1$) and the open shell singlet ($S = 0$) states using the relation

$$J = \frac{1}{2}[E(\mathrm{S} = 1) - E(\mathrm{S} = 0)] \quad (2)$$

It is well-known that the restricted Hartree−Fock method gives a good starting geometry but a rather bad total energy unless one uses a large basis set and resorts to post-Hartree−Fock treatment. The unrestricted Hartree−Fock method is more useful in this context.[17b−d] Nevertheless, because it is based on a single determinant wave function, it cannot properly describe the open shell singlet state in a biradical. This calls for a multideterminant approach that becomes computationally intractable as the size of the system increases. To overcome these difficulties, Noodleman[18] proposed the broken symmetry (BS) approach within the framework of density functional theory (DFT). The BS state is an average of low- and high-spin states and is described by a single determinant wave function. Noodleman's method is computationally affordable and yields

dx.doi.org/10.1021/jp402756j | J. Phys. Chem. A 2013, 117, 8609−8622

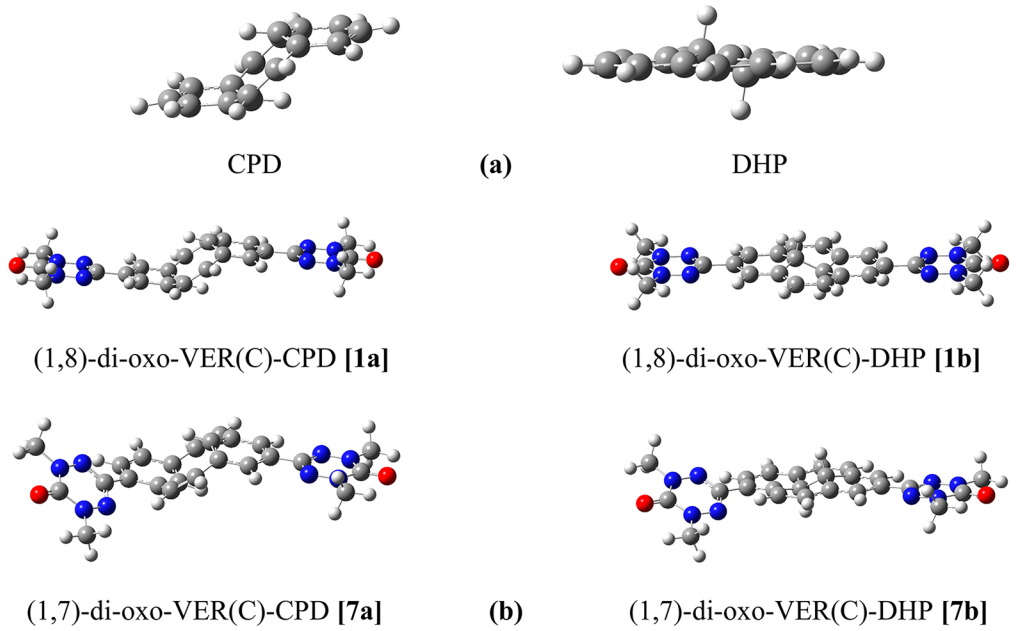

Figure 4. Optimized molecular geometries of (a) 15,16-dihydro-CDP and 15,16-dihydro-DHP, both having singlet ground states, and (b) (1,8)-dioxo-VER(C)−CPD [**1a**], (1,8)-dioxo-VER(C)−DHP [**1b**], (1,7)-dioxo-VER(C)−CPD [**7a**], and (1,7)-dioxo-VER(C)−DHP [**7b**] in their triplet states. The stepped up structures of the CPD isomers are evident.

good results. The ideal value of the average of the S^2 operator is 2 for the triplet state and 1 for the BS solution for a diradical. However, a pure $\langle S^2 \rangle$ is rarely obtained from an unrestricted calculation, except when the state is singlet and the calculation becomes effectively restricted. The use of a spin projection technique can make the computations more reliable. Noodleman suggested the estimation of J from the relation

$$J^{\mathrm{N}} = \frac{({}^{\mathrm{DFT}}E_{\mathrm{BS}} - {}^{\mathrm{DFT}}E_{\mathrm{T}'})}{1 + \mathrm{S_{ab}}^2} \quad (3)$$

where ${}^{\mathrm{DFT}}E_{\mathrm{T}'}$ is the energy of the triplet wave function that can be built from the BS orbitals, and $\mathrm{S_{ab}}$ is the overlap between the magnetically active orbitals a and b. For practical considerations, ${}^{\mathrm{DFT}}E_{\mathrm{T}'}$ can be replaced by the calculated energy of triplet ${}^{\mathrm{DFT}}E_{\mathrm{T}}$, since the spin contamination in the triplet is normally quite small. Equation 3 becomes unreliable as the overlap between the magnetic orbitals increases. A more reliable expression for the magnetic exchange coupling constant was devised by Yamaguchi:[19]

$$J^{Y} = \frac{({}^{\mathrm{DFT}}E_{\mathrm{BS}} - {}^{\mathrm{DFT}}E_{\mathrm{T}})}{\langle \mathrm{S}^2 \rangle_{\mathrm{T}} - \langle \mathrm{S}^2 \rangle_{\mathrm{BS}}} \quad (4)$$

This equation takes care of the spin contamination effects in calculated broken symmetry and triplet states.

We have used eq 4 to estimate the magnetic exchange coupling constant from unrestricted DF calculations using the hybrid B3LYP functional.[20] This functional has been chosen because it retains a significant amount of Hartree−Fock exchange, thereby limiting the self-interaction error. This functional is known to be very useful for calculation of J. The unrestricted procedure has been used to get spin-polarized states. Optimization of molecular geometry in the triplet state has been done using 6-311G(d,p) basis set. Single-point calculations on both triplet and broken symmetry states have been carried out with the 6-311++G(d,p) basis set using the optimized geometry of the triplet. All calculations have been done using Gaussian03 (G03)[21a] and Gaussian09 (G09)[21b] quantum chemical computation packages.

The Yamaguchi equation corrects the calculated energy difference for the effect of spin contamination; however, the deviation of $\langle S^2 \rangle$ from its ideal value also affects the geometry optimization procedure. A large contamination can significantly distort the equilibrium geometry. Kitagawa et al.[22] investigated this issue and proposed a geometry correction procedure based on spin projection techniques. Fortunately, in this work most of the diradicals show calculated $\langle S^2 \rangle$ to within ±5% of the ideal value and $\Delta\langle S^2 \rangle$ approximately equal to 1. Hence, the optimized molecular geometries and the associated energy differences may be taken as fairly correct.

The use of the projection technique together with the broken symmetry approach is no doubt the right way to proceed; however, there are several other options available in the form of the so-called HDVV spin Hamiltonian and effective Hamiltonian theories that are especially applicable to transition metal compounds.[23]

To test whether photochromic behavior is possible for the diradicals, spectroscopic transition energies and oscillator strengths have been calculated. We have used time-dependent density functional theory (TDDFT)[24] and the 6-311++G(d,p) basis set for this purpose. The TDDFT singlet calculation in Gaussian is based on the restricted RB3LYP methodology. This poses some problems for the diradicals, because in both G03 and G09, the calculation assumes a closed shell ground state and finds excited singlet states. Therefore, it creates an artificial red shift when the diradical ground states are open shell singlets, as the TDDFT ground state energy ($E_{\mathrm{g}}^{\mathrm{TD}}$) is greater than the energy of the open-shell ground state (E_{S}). The triplet TDDFT calculation does not suffer because all the computed states are of type $\alpha\alpha$; therefore, all TDDFT calculations have been performed on triplet states using triplet geometry.

We have estimated the open shell singlet energy from the modified Yamaguchi equation

dx.doi.org/10.1021/jp402756j | J. Phys. Chem. A 2013, 117, 8609−8622

Table 1. Single-Point Energies of Triplet and Broken Symmetry State and Calculated J Values Obtained Using the UB3LYP/6-311++G(d,p) Method[a]

molecule	E_T (a.u.) ($\langle S^2\rangle$)	E_{BS} (a.u.) ($\langle S^2\rangle$)	J (cm^{-1})
	Group a		
(1,8)-dioxo-VER(C)−CPD [**1a**]	−1516.4901374 (2.0469)	−1516.4901756 (1.0494)	−4.4
(1,8)-dioxo-VER(C)−DHP [**1b**]	−1516.5212432 (2.0460)	−1516.5218291 (**1.1039**)	**−136.5**
(1,8)-dioxo-VER(C)−15,16-dinitrile-CPD [**2a**]	−1701.0075084 (2.0486)	−1701.0075612 (1.0539)	−11.6
(1,8)-dioxo-VER(C)−15,16-dinitrile-DHP [**2b**]	−1701.0236114 (2.0461)	−1701.0242459 (**1.1125**)	**−149.2**
	Group b		
1-oxo-VER(N)−8-oxo-VER(C)−CPD [**3a**]	−1516.4854262 (2.0468)	−1516.4853512 (1.0434)	16.4
1-oxo-VER(N)−8-oxo-VER(C)−DHP [**3b**]	−1516.5190703 (**2.1218**)	−1516.5175842 (1.0474)	**303.6**
1-oxo-VER(N)−8-oxo-VER(C)−15,16-dinitrile-CPD [**4a**]	−1701.0038839 (2.0493)	−1701.0037616 (1.0448)	26.7
1-oxo-VER(N)−8-oxo-VER(C)−15,16-dinitrile-DHP [**4b**]	−1701.0210276 (**2.1325**)	−1701.0194622 (1.0493)	**317.2**
	Group c		
(1,8)-dioxo-VER(N)−CPD [**5a**]	−1516.4803923 (2.0394)	−1516.4805594 (1.0399)	−36.7
(1,8)-dioxo-VER(N)−DHP [**5b**]	−1516.5135125 (2.0345)	−1516.5159607 (1.0522)	**−546.9**
(1,8)-dioxo-VER(N)−15,16-dinitrile-CPD [**6a**]	−1700.9996560 (2.0410)	−1700.9999598 (1.0411)	−66.7
(1,8)-dioxo-VER(N)−15,16-dinitrile-DHP [**6b**]	−1701.0147506 (2.0352)	−1701.0174427 (1.0610)	**−606.5**
	Group d		
(1,7)-dioxo-VER(C)−CPD [**7a**]	−1516.4844413 (2.0474)	−1516.4844242 (1.0458)	3.7
(1,7)-dioxo-VER(C)−DHP [**7b**]	−1516.5145360 (2.0721)	−1516.5143141 (1.0489)	47.6
(1,7)-dioxo-VER(C)−15,16-dinitrile-CPD [**8a**]	−1701.0002887 (2.0483)	−1701.0002734 (1.0470)	3.4
(1,7)-dioxo-VER(C)−15,16-dinitrile-DHP [**8b**]	−1701.0167129 (2.0804)	−1701.0164394 (1.0490)	58.2
	Group e		
(1,7)-dioxo-VER(N)−CPD [**9a**]	−1516.4784807 (2.0410)	−1516.4784436 (1.0392)	8.1
(1,7)-dioxo-VER(N)−DHP [**9b**]	−1516.5095768 (2.0790)	−1516.5091420 (1.0532)	93.0
(1,7)-dioxo-VER(N)−15,16-dinitrile-CPD [**10a**]	−1700.9937807 (2.0429)	−1700.9937367 (1.0406)	9.6
(1,7)-dioxo-VER(N)−15,16-dinitrile-DHP [**10b**]	−1701.0087418 (2.0903)	−1701.0081470 (1.0541)	126

[a]Larger deviations of $\langle S^2\rangle$ and larger J values are shown in bold face.

$$E_S = \frac{(E_{BS}\langle S^2\rangle_T - E_T\langle S^2\rangle_{BS})}{\langle S^2\rangle_T - \langle S^2\rangle_{BS}} \quad (5)$$

The correction to the calculated TDDFT excitation energy is given by

$$\Delta E_{ex} = E_g^{TD} - E_S \quad (6)$$

From our previous work in the subject, however, we found that the shift is not very large when the spacer is CPD or DHP.[6a−c] If the calculated transition bands closely correspond to those for CPD and DHP, are considerably higher in energy than the thermal activation barriers (20−25 kcal mol^{-1}), and sufficiently intense, there is a strong likelihood that the diradical pairs would be photochromic isomers. This is, of course, subject to the assumption that the barrier to ground state interconversion does not greatly change by radical substitutions.

RESULTS AND DISCUSSION

Diradical Systems. It is well-known experimentally as well as theoretically that CPD is a stepped molecule and DHP has an extensive conjugation to become rather planar with the substituents R projecting out of plane (see Figure 4a). In case more (radical) substituents are inserted in positions such as (p,$\acute{p}$) or (1,8) and (p,m') or (1,7), they may be twisted out of the plane of benzenoid rings and show a nonzero dihedral angle, as evident from the optimized geometries of two diradical pairs in Figure 4b.

The molecular geometries optimized at the UB3LYP/6-311G(d,p) level for the triplet state are shown in Figure S1 of the Supporting Information. Total energies for triplet and broken symmetry states from single point calculations using the triplet-optimized molecular geometries and 6-311++G(d,p) basis set are given in Table 1. The calculated J values are also shown in this table.

Coupling Constant. The calculated J values vary in the range from −606 to 317 cm^{-1}. These are positive for diradicals belonging to groups b, d, and e in Table 1. No spin crossover is observed here, but this need not be disheartening because one can still find photomagnetic switching. The J values of the CPD diradicals are small in magnitude, whereas for the DHP derivatives, the coupling constants are substantially large except for the DHP diradicals of group d.

Somewhat large spin contamination is observed in the broken symmetry state of the DHP diradicals belonging to group a in Table 1 [**1b** and **2b**] and triplet state of DHP diradicals of group b [**3b** and **4b**]. This indicates that the J calculated for DHP forms of groups a and b in Table 1 are quantitatively less reliable. These are strongly coupled diradicals, group a with intramolecular antiferromagnetic interaction and group b with ferromagnetic coupling. However, group c consists of more strongly antiferromagnetically coupled DHP diradicals with less spin contamination in the BS state. Apparently, there is no direct connection between the spin contamination and the largeness of J for such systems. In fact, the DHP systems of groups d and e exhibit significantly weaker ferromagnetic coupling, although they are associated with smaller-range spin contamination effects with $\Delta\langle S^2\rangle$ nearly equal to 1.

Using B3LYP is a valid option, although this generally tends to overestimate the J values. Therefore, we have repeated the single-point calculations using a more modern functional, namely, M06-2X, which includes dispersion corrections.[25] M06-2X has a good response under dispersion forces. To compare, the s6 scaling factor on Grimme's long-range dispersion correction is 0.06 for M06-2X and 1.05 for B3LYP. M06-2X also has a healthy amount

dx.doi.org/10.1021/jp402756j | J. Phys. Chem. A 2013, 117, 8609−8622

Table 2. Single Point Triplet and Broken Symmetry Energy Values from the M062X/6-311++G(d,p) Scheme[a]

system	E_T (a.u.) ($\langle S^2 \rangle$)	E_{BS} (a.u.) ($\langle S^2 \rangle$)	$J_{M06\text{-}2X}$ (cm^{-1})	J_{UB3LYP} (cm^{-1})
3a	−1515.8840391 (2.056430)	−1515.8839939 (1.024703)	10.1	16.4
3b	−1515.9063566 (2.174590)	−1515.9046646 (1.06338)	334.2	303.6
4a	−1700.3582998 (2.059308)	−1700.3582207 (1.056186)	17.3	26.7
4b	−1700.3641441 (2.196035)	−1700.3622724 (1.068157)	364.2	317.2
5a	−1515.8793070 (2.050196)	−1515.8793896 (1.051391)	− 18.0	−36.7
5b	−1515.901637 (2.047480)	−1515.9037819 (1.128307)	− 512.1	−546.9
6a	−1700.3020255 (2.050014)	−1700.3021965 (1.051275)	− 37.6	−66.7
6b	−1700.3586520 (2.048191)	−1700.3611705 (1.149204)	− 614.8	−606.5

[a]We have retained the UB3LYP/6-311G(d,p) optimized geometry for the triplet in all these calculations.

Table 3. M06-2X Energies of Triplet State with Optimized Geometry from 6-311G(d,p) Basis Set, and Single-Point Triplet and Broken Symmetry Energies Obtained Using 6-311++G(d,p) Bases

		6-311++G(d,p) single point energy		
system	6-311G(d,p) optimized geometry E_T (a.u.) ($\langle S^2 \rangle$)	E_T (a.u.) ($\langle S^2 \rangle$)	E_{BS} (a.u.) ($\langle S^2 \rangle$)	$J_{M06\text{-}2X}$ (cm^{-1})
3a	−1515.865793 (2.054037)	−1515.8855079 (2.053949)	−1515.8854716 (1.052623)	8.0
3b	−1515.8881641 (2.14873)	−1515.9077656 (2.149096)	−1515.9063849 (1.056708)	277.5
5a	−1515.8610316 (2.048341)	−1515.8812043 (2.048726)	−1515.881272 (1.049602)	−14.9
5b	−1515.8831182 (2.046588)	−1515.9035231 (2.046865)	−1515.9051214 (1.107081)	−373.3

(54%) of Hatree-Fock exchange that helps in keeping down self-interaction errors. The $J_{M06\text{-}2X}$ values reported in Table 2 for the most strongly coupled diradicals (**3a**, **3b**, **4a**, and **4b** for $J > 0$; **5a**, **5b**, **6a**, and **6b** for $J < 0$) are obtained from the M06-2X/6-311++G(d,p) level, whereas retaining the UB3LYP/6-311G(d,p) optimized triplet geometries. It is clearly borne out that the magnetic exchange coupling constant for CPD diradicals is almost half of J_{UB3LYP}. The calculated J values remain more or less unaltered, to within ±10%, for DHP diradicals.

The optimized geometries obtained from using M062X and B3LYP functionals and the associated total energies show significant variation only when there is a large contribution from dispersive effects. These effects also tend to reduce the absolute magnitude of coupling constant. These phenomena are evidenced here for the diradicals with CPD spacer, where, because of stacking, conjugation becomes less extensive and dispersive interaction increases. From Table 3, we indeed find that the use of M06-2X/6-311G(d,p) optimized triplet geometries leads to a further decrease in the J values for the CPD diradicals. For instance, for **3a**, J_{UB3LYP} = 16.4 cm^{-1} (Table 1), $J_{M06\text{-}2X}$ = 10.1 cm^{-1} at the UB3LYP geometry (Table 2), and $J_{M06\text{-}2X}$ = 8.0 cm^{-1} at the M06-2X geometry (Table 3). For **5a**, the same quantities are −36.7, −18.0, and −14.9 cm^{-1}, respectively. It is important to notice that under geometry optimization, the DHP diradicals also show about 10−30% reduction in the J value when calculated with the M06-2X functional instead of the B3LYP.

Spin Density Distribution. In all the cases, the $|J|$ value of the CPD derivative is much less than that for the DHP derivative. This is due to the fact that DHP's being almost planar (with 14 conjugated π electrons) offers a facile means of spin transport, whereas in CPD, the conjugation is less because its stepped structure (two conjugated benzene rings with 6 π electrons in each) and spin conjugation are hindered. This has been discussed in detail in refs 6a−c. The effect of π-conjugation can be easily visualized from the spin density distributions for **4a** and **4b** in Figure 5. Both diagrams reveal systematic spin alternation, thereby indicating a ferromagnetically coupled ground state. The much-reduced spin densities in the middle of **4a** arise from a decreased π-conjugation and lead to a significantly small coupling constant. Spin density diagrams for all the species are given in Figure S2 of the Supporting Information.

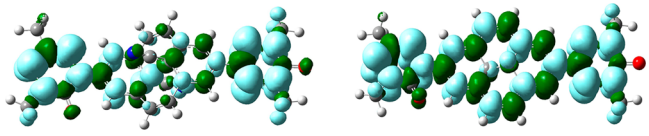

Figure 5. Spin density plots with isovalue 0.0008 for **4a** (left) and **4b** (right) in their triplet states.

Spin Alternation Rule. There is an opposite spin density region between N2 and N4 in the oxoverdazyl group with the spin on both nitrogen atoms in the same direction. This property of the o-VER group helps one to follow the spin alternation rule. With the help of Supporting Information Figure S2, it can be shown that the calculated coupling constants for all diradicals are in accordance with this rule. The spin alternation schemes for the five groups of species are illustrated in Figure 6.

It is easy to observe that on using either the C- or the N-terminal of the o-VER group on both sides of the coupler, the J value comes out to be negative for 1,8- radicalization, whereas a mixed arrangement gives a positive J value. The situation is reversed for the 1,7-diradicals. The 1,8-diradicals have large coupling constants in the DHP form. This happens because spin oscillations along the two possible routes reaching position 8 constructively superpose on each other because their phases are equal. The 1,7-diradicals have somewhat out-of-phase interference that is less constructive, and this leads to a drastically reduced coupling constant.

SOMO Effect. It is possible to predict the nature of ground state from SOMO plots, as proposed by Borden and Davidson.[17] According to them, when the SOMOs are disjoint, the singlet state is the ground state. If the SOMOs extend over nondisjoint groups of atoms, then in the triplet state, some of the atoms have the electrons of parallel spin, which contributes to the exchange interaction that is negative, and the triplet lies below the singlet state in energy. However, this comes with a caveat. It is possible to find the SOMOs as nondisjoint in some cases, but a careful look may reveal that their orthogonal linear combinations can be really disjoint.

dx.doi.org/10.1021/jp402756j | J. Phys. Chem. A 2013, 117, 8609−8622

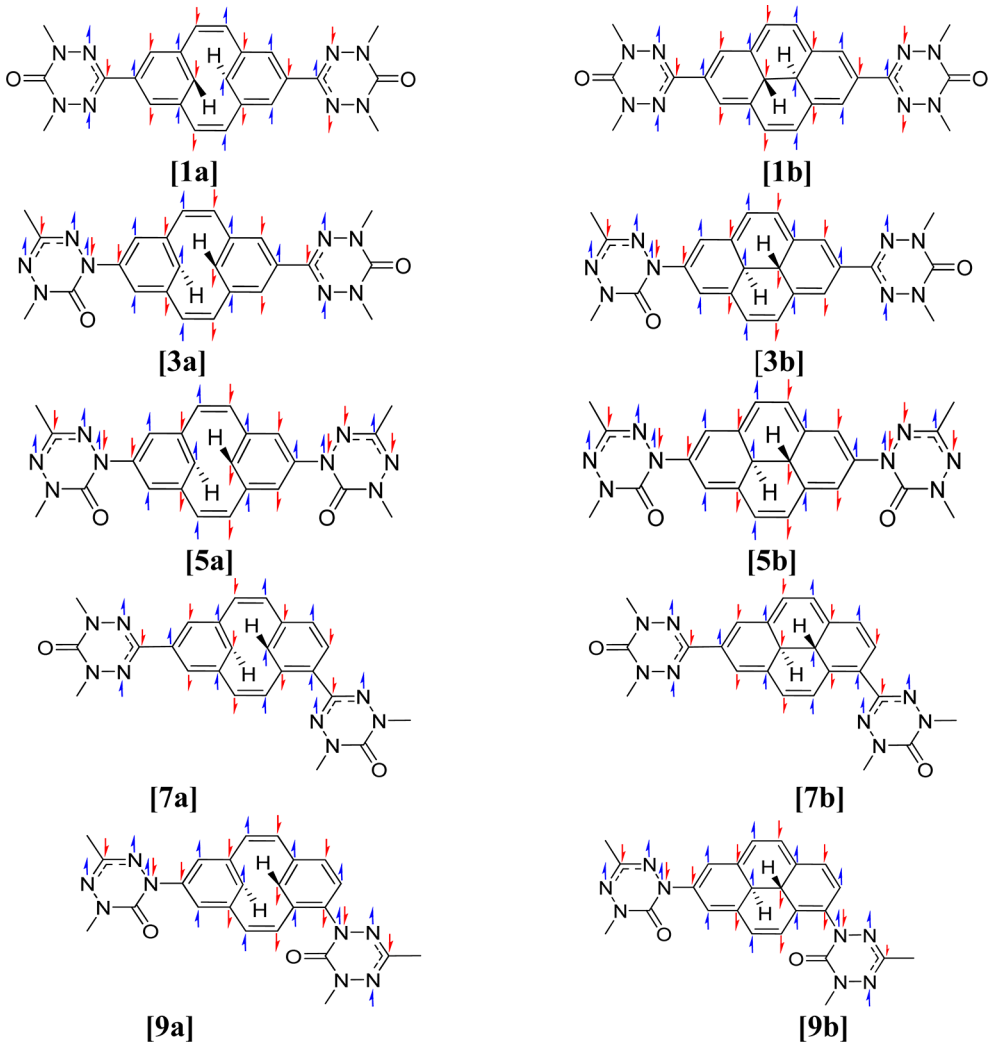

Figure 6. The diagrams showing spin alternation rule in the systems. (ChemDraw software has been used to draw these diagrams.)

It is evident from Figure 7 that the linear combination of the SOMOs produces disjoint diagrams for diradical **2a** and **2b.** Thus, these *p*,*ṕ*-dioxoverdazyl diradicals have singlet ground states. This is in conformity with *J* equal to −12 and −149 cm^{-1}, respectively, in Table 1. For the *p*,*ṕ*-mixed dioxoverdazyl diradicals **3a** and **3b**, SOMOs are clearly nondisjoint, and any linear combination thereof still gives rise to a pair of nondisjoint orbitals. Thus, these diradicals have positive *J* values, 16 and 304 cm^{-1}, respectively, corresponding to triplet ground states. Similar observations have been made for all other diradicals in this work, and the relevant SOMO diagrams have been included in Figure S3 of the Supporting Information.

Dihedral Angle. The dihedral angle also has a considerable influence on the magnetic exchange interaction, but the trend is generally masked here because there are four spacers (CPD and DHP, with R = H, CN), and the diradicals have been prepared by using three different radical centers at two different relative positions. There are not sufficient numbers of compounds with similar structural and topological interactions to observe a trend.

Different radical center combinations and their positions produce magnetic interaction of different strengths.[26] The problem becomes more complicated because the CPD diradicals have very weak magnetic coupling. Nevertheless, a qualitative trend is visible for the DHP diradicals: when the dihedral angles are small, the *J* values are large in magnitude. The latter happens because a greater conjugation between the spacer and radical centers facilitates the through-bond spin interaction.

The dihedral angle of each radical center with CPD/DHP is defined in Figure 8. The calculated angles are given in Table 4. Three geometrical effects are noticed here: First, for the 1,8 radical substitution on CPD or DHP (**1**, **2**), the o-VER(C) linkage leads to almost zero dihedral angle; that is, the radical center is coplanar with the attached benzene ring. Second, because the chosen configuration with o-VER(N) link has an oxygen substituent that crowds the pyrene ring, it gives rise to a dihedral angle that varies from 16° to 35° for the same position of radical centers; (**3**, **4** versus **1**, **2**; **5**, **6** versus **3**, **4**). Third, a substitution at position 7 is associated with a further increase in the dihedral angle by approximately 30°; (**7**, **8** versus **1**, **2**; **9**, **10** versus **5**, **6**).

Influence of Nitrile Group. It is observed from the calculated *J* values that −CN groups at the 15, 16 positions have a significant influence on the magnetic exchange coupling for 1,8- radicalization on the CPD molecule. The magnitude of *J* for the CPD molecule increases on replacing the H atoms in the 15, 16 positions with CN groups (**1a**−**6a**), whereas the effect is less prominent in the corresponding DHP diradicals (**1b**−**6b**). This is due to the fact that the nitrile group is so positioned that it can conjugate well with the phenyl ring to which it is attached in CPD diradicals. This has a stabilizing effect on the ground state

dx.doi.org/10.1021/jp402756j | J. Phys. Chem. A 2013, 117, 8609−8622

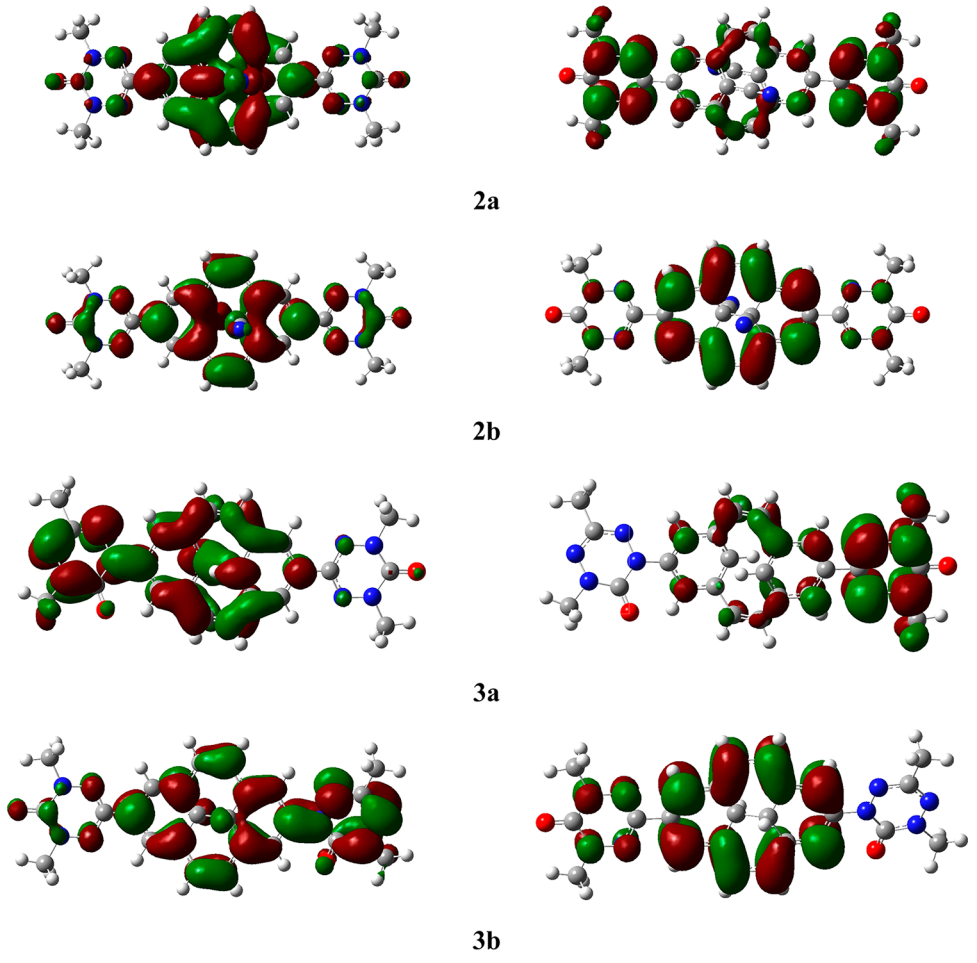

Figure 7. SOMO 1 and SOMO 2 plots for diradicals **2a** and **2b** (both antiferromagnetically coupled) and **3a** and **3b** (both ferromagnetically coupled).

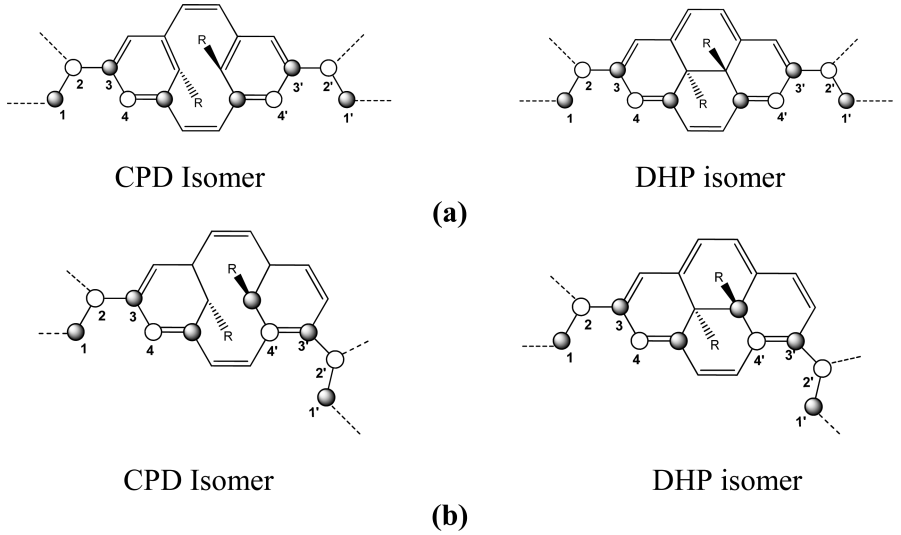

Figure 8. Dihedral angles for (a) 1,8- radicalization (linear system) and (b) 1,7- radicalization (bent system).

and tends to enlarge the coupling constant by greater recovery of conjugation between the two phenyl rings. In the DHP form, the nitrile groups become almost orthogonal to the phenyl rings, and the effect is small. In the case of 1,7- radicalization, one radical center is already twisted out of plane such that the effect is largely subdued for the CPD diradicals. Thus, **7a** and **8a** have nearly equal *J* values, and the same is observed for **9a** and **10a**.

Electronic Transitions. Irradiation of CPD with light of wavelength <313 nm (>3.96 eV) converts it to DHP, whereas DHP converts into CPD at >365 nm (<3.40 eV).[13a,b] We have studied the UV−visible absorption properties of 15,16-dinitrile-CPD/DHP and the unsubstituted species in their singlet ground state and all the derivatives in their triplet ground states by TDDFT using 6-311++G(d,p) basis set. TDDFT calculations on

dx.doi.org/10.1021/jp402756j | J. Phys. Chem. A 2013, 117, 8609−8622

Table 4. Dihedral Angles in Degree from Optimized Triplet Geometry and the Corresponding Calculated *J* Values

system	(1−2−3−4)	(1′−2′−3′−4′)	J (cm^{-1})	system	(1−2−3−4)	(1′−2′−3′−4′)	J (cm^{-1})
[**1a**]	2.6	2.7	−4.4	[**1b**]	1.7	1.7	−136.5
[**2a**]	3.3	3.3	−11.6	[**2b**]	2.0	2.0	−149.2
[**3a**]	26.6	−2.8	16.4	[**3b**]	23.1	−1.5	303.6
[**4a**]	−22.7	−2.9	26.7	[**4b**]	16.3	−1.4	317.2
[**5a**]	27.1	26.9	−36.7	[**5b**]	−34.8	−34.9	−546.9
[**6a**]	−21.6	−21.7	−66.7	[**6b**]	−28.1	−28.0	−606.5
[**7a**]	−3.3	−34.0	3.7	[**7b**]	−1.7	−35.7	47.6
[**8a**]	−3.8	−32.2	3.4	[**8b**]	−1.7	−30.7	58.2
[**9a**]	−31.8	−58.0	8.1	[**9b**]	−31.1	−66.9	93
[**10a**]	−20.8	−55.8	9.6	[**10b**]	−24.8	−62.8	126

15,16-dinitrile-CPD and 15,16-dinitrile-DHP give excitation energies and oscillator strengths in good agreement with the observed values in ref 10. These are shown in Table 5. The

Table 5. Calculated and Experimental Excitation Energy and Oscillator Strength (extinction coefficient) of 15,16-Dinitrile-CPD and 15,16-Dinitrile-DHP[a]

15,16-dinitrile-CPD				15,16-dinitrile-DHP			
calcd		exptl[b]		calcd		exptl[b]	
nm	f	nm	ε	nm	f	nm	ε
223	*0.072*			229	0.011		
224	*0.176*	*225*	*30000*	323	0.886	331	87300
227	*0.086*			*369*	*0.273*	*367*	*34300*
234	*0.275*			*474*	*0.016*	*442*	*6400*
254	*0.195*					*528*	*80*
300	*0.156*	*282*	*9800*			*599*	*130*
304	*0.047*					*640*	*770*
		330	4800				
		367	1600				
407	0.023						

[a]The italic range is important for photoconversion. [b]In CH_2Cl_2, from ref 11.

calculated spectral data for the dihydrogen (that is, unsubstituted) CPD and DHP and their diradical derivatives **3a** and **3b** are compared in Table 6. The 50 lowest energy transitions have been considered for each species, and only the prominent ones are shown here. Supporting Information Table S3, S4, S5, and S6 contain the excitation energies and corresponding oscillator strengths obtained from the TDDFT calculations for all the diradicals.

It is important to realize that the n-π^* and $\pi-\pi^*$ transitions are active in photochromism, the $\sigma-\pi^*$ and $\sigma-\sigma^*$ being energetic enough to cleave a bond. When the radical centers are conjugated with the coupler, the π and π^* energy bands become wider. This leads to a general red shift in the $\pi-\pi^*$ and n$-\pi^*$ spectral bands. The HOMO−LUMO energy gap ($\Delta\varepsilon$) is given in Table S2 of the Supporting Information. It is observed that $\Delta\varepsilon$ for 15,16-dinitrile CPD is 3.64 eV, and the value decreases for the corresponding diradicals, the range being 2.04−2.62 eV for dinitrile derivatives. Similarly, $\Delta\varepsilon$ for 15,16-dinitrile DHP is 3.09 eV, and for the DHP-diradicals, $\Delta\varepsilon$ is found in the range 1.48−2.58 eV for dinitrile derivatives.

A blue shift also occurs for the higher energy transitions as the spectral line width increases. The transitions in general become more intense: this especially happens when a charge transfer transition of a radical center is mixed with the n$-\pi^*$ and $\pi-\pi^*$ transitions.

Table 6. Calculated Excitation Energy and Oscillator Strength of Unsubstituted CPD and DHP in Their Singlet Ground State and the Diradical Derivatives in Their Triplet Ground State Using 6-311++G(d,p) Basis Set[a]

CPD		[3a]		DHP		[3b]	
eV	f	eV	F	eV	f	eV	f
4.821	*0.008*	*4.614*	*0.037*			4.145	0.032
		4.516	*0.318*			3.942	0.011
		4.478	*0.050*			3.856	0.010
		4.469	*0.021*	3.870	0.954	3.788	0.044
4.419	*0.009*	*4.359*	*0.034*			3.754	1.348
		4.139	*0.027*			3.701	0.076
4.062	*0.279*	*4.095*	*0.460*			*3.452*	*0.022*
		4.022	*0.067*	*3.392*	*0.316*	*3.361*	*0.112*
3.359	0.006	3.491	0.019			*3.353*	*0.052*
		3.104	0.011			*3.180*	*0.020*
		3.021	0.024			*3.054*	*0.021*
		2.913	0.034			*3.041*	*0.083*
		2.805	0.029			*3.000*	*0.028*
		2.800	0.044			*2.885*	*0.042*
		2.364	0.107	*2.634*	*0.015*	*2.574*	*0.011*
						2.406	*0.205*
						2.322	*0.074*
						2.087	*0.070*
						1.809	*0.213*
						1.775	*0.022*
						1.248	*0.036*

[a]The range in italic is important for photoconversion.

TDDFT indeed yields a red shift for each radical substituted system. The calculated strongest transitions for both dihydrogen- and dinitrile-DHPs are found in the region 3.8−3.9 eV, whereas for most of the corresponding diradicals, the strongest excitations are calculated in the range 3.7−3.8 eV. For species **7b** and **8b**, the strongest excitations are found around 3.4 eV. A simple explanation seems to elude, but this can be viewed as an outcome of the spin-carrying N−C−N part of oxoverdazyl group being bonded to position 7 of the DHP ring system, which leads to a lowering of the π^* orbitals. The DHP red shift is quite large at the low energy range, but small for the most intense transitions.

In the case of the dihydrogen-CPD derivatives, however, the most prominent transitions occur more or less at the same energy (4.06 eV for the unsubstituted CPD) with a perceptively small blue shift, except for **7a** and **9a**, where a splitting is evident (see Supporting Information Table S3). These transitions increase in intensity from the parent pyrenes to the diradicals. The calculated most intense absorptions of interest occur for

dx.doi.org/10.1021/jp402756j | J. Phys. Chem. A 2013, 117, 8609−8622

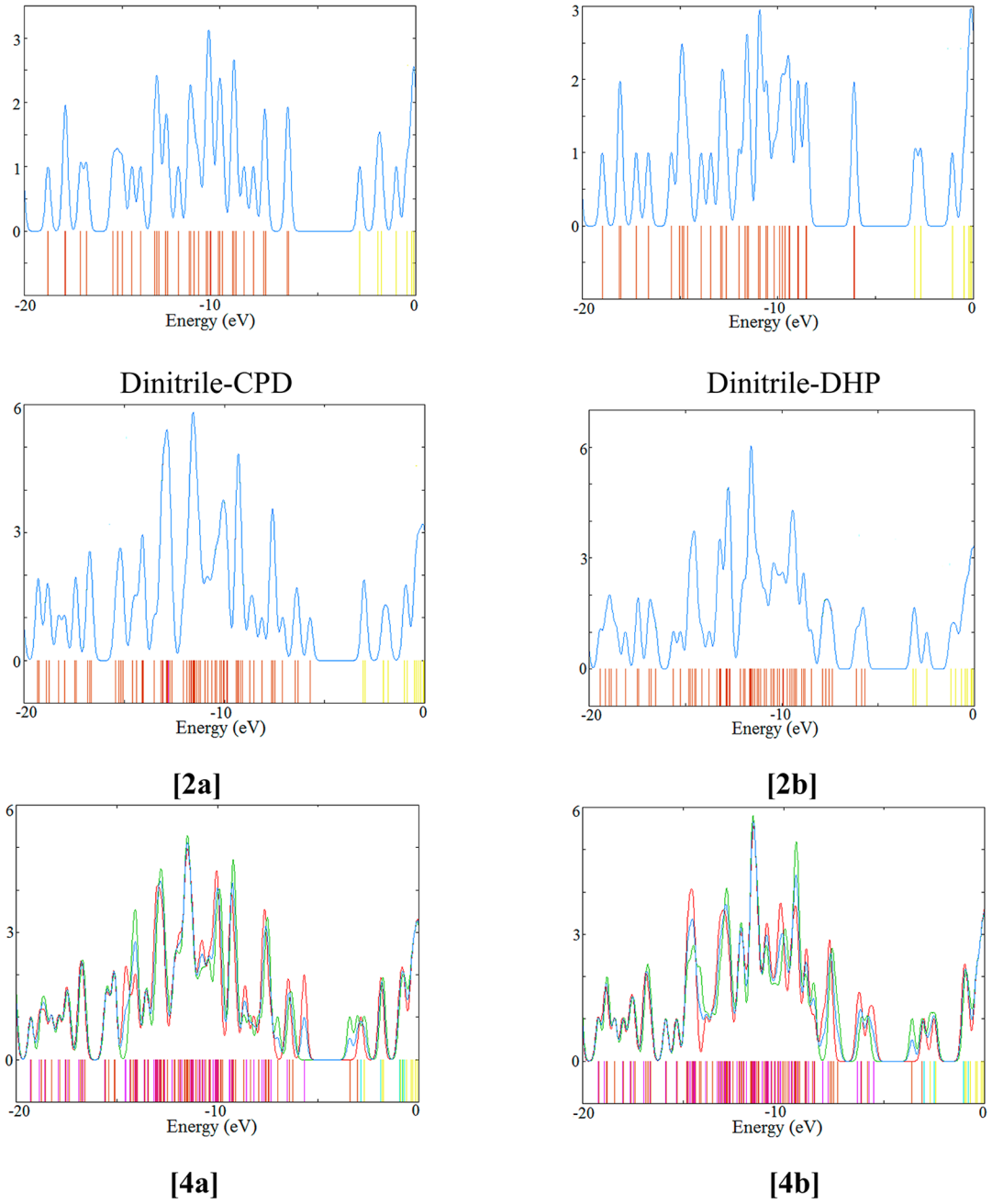

Figure 9. Typical density of states plots for the dinitrile derivatives: Singlet ground states for CPD and DHP, BS states for **2a** and **2b** (with $J < 0$), and triplet ground states for **4a** and **4b** (with $J > 0$). Only the total DOS spectrum is shown for singlet and BS states. For calculations with the triplet ground states, the notations are as follows: alpha DOS spectrum (primary red), beta DOS spectrum (green), total DOS spectrum (scaled by 0.5) (primary blue); alpha occupied orbitals (magenta), alpha virtual orbitals (light blue), beta occupied orbitals (dark red), beta virtual orbitals (yellow).

dinitrile-CPD in a range starting from 4.06 to 5.53 eV. For its radical derivatives, however, the number of intense absorptions is far less—one or two—in the range 3.8−4.3 eV. The bent species **8a** and **10a** are particularly affected, with **10a** having only one intense transition calculated at energy 2.48 eV. This is evidently an effect of the electron-pulling nitrile groups.

The transitions listed in Table 6 and the Supporting Information show that they have enough energy to go over the activation barrier, from the CPD-based diradical to the DHP-based diradical and vice versa. TDDFT also clearly shows an increase in bandwidth and the intensity build-up. Perhaps the red and blue shifts and the spreading of the bandwidth can be best visualized from the HOMO and LUMO regions (right end) of the density of states spectra shown in Figure 9 for the dinitrile isomers (CPD and DHP) and their diradical derivatives (**2a**, **2b**, **4a**, and **4b**). Other DOS spectra have been given in the Supporting Information (Figure S4).

Correction to Transition Energy. The TDDFT calculation, nevertheless, encounters another problem for the diradicals, as discussed in the earlier section. An artificial red shift is created for the singlet species. Because the calculations are performed on the T ↔ T transitions, the fake red shift is, indeed, equal to $J\langle S^2\rangle_T$, the difference of the calculated energy of triplet from the estimated energy of singlet. This is generally borne out by Supporting Information Tables S3−S6. CPD, DHP, and their dinitrile derivatives are closed-shell species. The diradicals **1a**, **1b**,

dx.doi.org/10.1021/jp402756j | J. Phys. Chem. A 2013, 117, 8609−8622

2a, **2b**, **5a**, **5b**, **6a**, and **6b** are open shell singlets, and the TDDFT excitation energies have been corrected for these. These corrections are shown in Table 7.

Table 7. Calculated Correction to TDDFT Excitation Energy for Diradicals with Singlet Ground States[a]

systems	TDDFT ground state energy in a.u. (E_g^{TD})	est ground state energy in a.u. (E_S)[b]	corr to TDDFT transition energy (eV)[c]
1a	−1516.469158	−1516.490216	0.5730
1b	−1516.521243	−1516.522516	0.0346
2a	−1701.007507	−1701.007617	0.0030
2b	−1701.023611	−1701.025002	0.0379
5a	−1516.480392	−1516.480733	0.0093
5b	−1516.513513	−1516.518583	0.1380
6a	−1700.999656	−1701.000276	0.0169
6b	−1701.014751	−1701.020375	0.1530

[a]This correction is equal to $J\langle S^2\rangle_T$, the difference between the calculated triplet energy and the estimated singlet energy. [b]Using eq 5. [c]Using eq 6.

The corrected transition energies are given in Table 8, where they have been compared with the transition energies for CPD, DHP, and their dinitrile derivatives. There are a number of prominent transitions at <313 nm for CPD diradicals and >365 nm for DHP diradicals. These all have energy much greater than the thermal activation barrier (about 1 eV) of the parent species.

Photomagnetic Properties. Because the singlet−triplet energy difference equals 2*J*, all the CPD compounds (with calculated intramolecular $|J| < 67\ cm^{-1}$) would be paramagnetic at room temperature ($k_BT \approx 207\ cm^{-1}$) because there would be comparable populations in the singlet and triplet states. The DHP diradicals with large negative coupling constants are predominantly diamagnetic species, whereas those with large positive *J* values form almost pure paramagnetic compounds. This indicates that activation by light would involve a drastic change in the molar susceptibility of these species in solution, thin film, or a matrix.

The trend of the photomagnetic properties has been discussed in detail for stilbene on the basis of the diradicals in ref 27, so an abbreviated discourse is presented here. The molar paramagnetic susceptibility of an ensemble of these molecules is given by the Bleaney−Bowers equation,[28]

$$\chi_M = \frac{3.00067}{(3 + e^{-2.8773J/T})T} \quad (7)$$

where χ_M is in units of $cm^3\ mol^{-1}$, *J* is in cm^{-1}, and *T* is in Kelvin.[27] Diradical **4b** has the largest positive *J* (317 cm^{-1}), and **6b** has the largest negative *J* (−607 cm^{-1}). The corresponding CPD forms **4a** and **6a** have much smaller coupling constants (27 and −67 cm^{-1}, respectively). Therefore, typical plots of χ_M versus *T* and $\chi_M T$ versus *T* for the pairs **4a**, **4b** and **6a**, **6b** are shown in Figure 10. In addition, the estimated change in molar susceptibility arising from light-activated interconversion at room temparature is exhibited in Table 9. All CPD isomers have χ_M varying in the range $2.1-2.7 \times 10^{-3}$ cc mol^{-1}. The photoconversion of CPD into DHP is predicted to be associated with an appreciable decrease of χ_M for the (1,8)-dioxo-Verdazyl(C) species **1** and **2**, an appreciable increase for (1,8)-mixed species **3** and **4** and an almost total wipeout for the (1,8)-dioxo-Verdazyl(N) species **5** and **6**. Table 9 also reveals that the molecules belonging to groups a and b in Table 1 can be generally classified as photomagnetic. Molecules of group c are almost pure photomagnetic switches at room temperature, which can also be directly guessed from Figure 10.

CONCLUSIONS

Quantum chemical calculations have been used to investigate 10 pairs of diradicals. These diradicals have been designed by using the photoswitching pyrene molecules, namely, CPD and DHP, and their dinitrile derivatives as spacers. The oxoverdazyl group has been used as radical centers. We have considered substitution

Table 8. Corrected excitation energies of prominent and relevant transitions for systems with singlet ground states[a]

system	TDDFT excitation energy (eV)	oscillator strength (f)	corr excitation energy (eV)	activation energy (excitation energy for photoconversion), eV
CPD (dihydrogen)	4.062	0.279		∼0.997[b] (>3.961[c])
1a	4.179, 4.467	0.413, 0.292	4.752, 5.040	
5a	4.080	0.456	4.089	
DHP (dihydrogen)	3.392	0.316	3.392	∼1.097[b] (<3.397[c])
1b	2.250, 2.449, 3.006, 3.148, 3.296	0.156, 0.323, 0.131, 0.145, 0.135	2.290, 2.489, 3.046, 3.188, 3.336	
5b	1.816,2.173, 3.170, 3.392	0.304, 0.147, 0.203, 0.054	1.954, 2.311, 3.308, 3.530	
CPD (dinitrile)	4.133, 4.881, 5.298, 5.462, 5.535, 5.560	0.156, 0.195, 0.275, 0.086, 0.176, 0.072	4.133, 4.881, 5.298, 5.462, 5.535, 5.560	1.098[d] (>3.961[c])
2a	3.964, 4.193, 4.236	0.220, 0.184, 0.418	3.967, 4.196, 4.239	
6a	4.145, 4.186, 4.271, 4.418	0.161, 0.084, 0.062, 0.054	4.162, 4.203, 4.288, 4.435	
DHP (dinitrile)	3.360	0.273	3.360	1.581[d] (<3.397[c])
2b	2.274, 2.662, 2.708, 3.179, 3.363	0.244, 0.282, 0.077, 0.162, 0.052	2.314, 2.702, 2.748, 3.219, 3.403	
6b	1.917, 2.034, 2.289, 2.987, 3.029, 3.427	0.344, 0.199, 0.064, 0.102, 0.137, 0.123	2.070, 2.187, 2.442, 3.140, 3.182, 3.580	

[a]CPD, DHP, and their dinitrile derivatives are closed-shell species and needed no correction. The diradicals included here are open-shell singlets, and the TDDFT excitation energies have been corrected. [b]Ref 13a. [c]Ref 13b. [d]Ref 12.

dx.doi.org/10.1021/jp402756j | J. Phys. Chem. A 2013, 117, 8609−8622

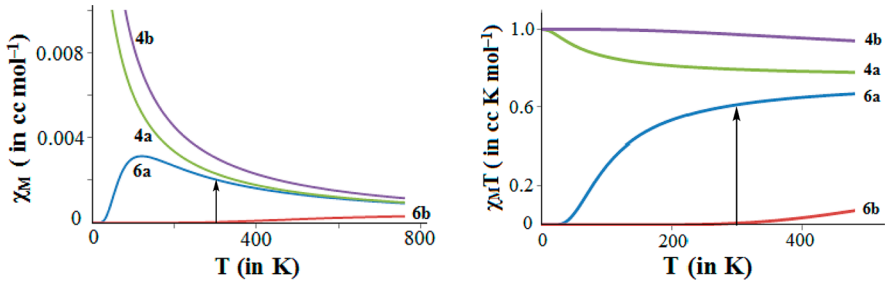

Figure 10. Plots of χ_M versus T and $\chi_M T$ versus T for diradicals **4a**, **4b** ($J > 0$) and **6a**, **6b** ($J < 0$). Compound **4b** would be strongly paramagnetic, and **6b**, practically diamagnetic. The change from **6b** to **6a** (photomagnetic switch) has been qualitatively illustrated by vertical arrows.

Table 9. Molar Susceptibility for Paramagnetic Solids at Room Temperature As Obtained from eq 7 Using the *J* Values Reported in Table 1

CPD isomer	χ_M (10^{-3} cc mol^{-1})	DHP isomer	χ_M (10^{-3} cc mol^{-1})
[**1a**]	2.5	[**1b**]	1.5
[**2a**]	2.4	[**2b**]	1.4
[**3a**]	2.6	[**3b**]	3.3
[**4a**]	2.7	[**4b**]	3.3
[**5a**]	2.3	[**5b**]	0.05
[**6a**]	2.1	[**6b**]	0.03
[**7a**]	2.5	[**7b**]	2.8
[**8a**]	2.5	[**8b**]	2.8
[**9a**]	2.6	[**9b**]	3.0
[**10a**]	2.6	[**10b**]	3.1

at 1,7 as well as 1,8 positions on the pyrene ring. Both C-linkage and connection through N atom have been taken into account.

The density functional methodology has been used to study the pyrenes and their diradicals. We have used the hybrid B3LYP functional in the unrestricted formulation. The basis sets chosen were 6-311G(d,p) for optimization of molecular geometry in the triplet state and 6-311++G(d,p) for single-point calculations on triplet as well as broken symmetry states using the optimized triplet geometry. We have also shown the effect of using a more modern functional, namely, M06-2X. The latter generally provides a smaller J value.

The favored ground state for the diradical is always in accordance with the spin alternation rule[16] and the nondisjoint SOMO effect.[17a,b] Because of the nearly planar geometry of the dihydropyrene derivatives, which allows much more extensive π-conjugation as compared with cyclophenadiene, the calculated magnetic exchange coupling constant is much larger for the DHP-coupled diradicals than the CPD-spaced derivatives. Substitution at position 7 on the pyrene ring gives rise to a larger dihedral angle and diminishes the coupling constant. The dinitrile substitution makes the ground state relatively more stable and increases the coupling constant. TDDFT spectra for the diradicals are red-shifted, broader, and more intense than the spectra of parent pyrenes.

Through our analysis, we have shown that it is possible to design diradicals that have intramolecular ferromagnetic (or antiferromagnetic) interaction with a large positive (or negative) J value. In addition, large J value differences between the photochromic isomers (up to 540 cm^{-1}) can be obtained. Coupled with good spectroscopic properties, it enables us to identify useful photomagnetic switches such as **5** and **6**, although no direct spin crossover has been theoretically observed for any of the diradicals.

■ ASSOCIATED CONTENT

Supporting Information

Log files of all calculations, optimized molecular geometries, spin density plots, SOMO plots, density of state plots, spin density on nitrogen atoms (table), HOMO−LUMO energies, and excitation wavelengths and oscillatory strengths. This material is available free of charge via the Internet at http://pubs.acs.org.

■ AUTHOR INFORMATION

Corresponding Author

*E-mail: sndatta@chem.iitb.ac.in.

Notes

The authors declare no competing financial interest.

■ ACKNOWLEDGMENTS

T.S. and S.N.D. are grateful to DST Grant SR-S1-PC-19-2010 for financial support of this work. A.K.P. and S.N.D. thank DST Grant INT-Spain-P42-2012 for financial support. S.H. thanks UGC for a research fellowship. I.A.L. thanks a CSIR-SRF fellowship for financial support. We acknowledge IIT Bombay computer center for making their facilities available to us.

■ REFERENCES

(1) (a) Iwamura, H.; Koga, N. Molecular Approaches to Photomagnetic Materials. Metal-Dependent Regiospecificity in the Exchange Coupling of Magnetic Metal Ions with the Free Radical Substituents on Pyridine Base Ligands. *Pure Appl. Chem.* **1999**, *71*, 231−238. (b) Einaga, Y. Photo-Switching Magnetic Materials. *J. Photochem. Photobiol. C* **2006**, *7*, 69−88. (c) Gütlich, P.; Garcia, Y.; Woike, T. Photoswitchable Coordination Compounds. *Coord. Chem. Rev.* **2001**, *219−221*, 839−879. (d) Bleuzen, A.; Marvaud, V.; Mathoniere, C.; Sieklucka, B.; Verdaguer, M. Photomagnetism in Clusters and Extended Molecule-Based Magnets. *Inorg. Chem.* **2009**, *48*, 3453−3466. (e) Dupouy, G.; Triki, S.; Marchivie, M.; Cosquer, N.; Gomez-Garcia, C. J.; Pillet, S.; Bendeif, E. -E.; Lecompte, C.; Asthana, S.; Letard, J.-F. Cyanocarbanion-Based Spin-Crossover Materials: Photocrystallographic and Photomagnetic Studies of a New Iron (II) Neutral Chain. *Inorg. Chem.* **2010**, *49*, 9358−9368.

(2) (a) Irie, M. Photochromism: Memories and Switches − Introduction. *Chem. Rev.* **2000**, *100*, 1683−1684. (b) Bouas-Laurent, H.; Dürr, H. Organic Photochromism. *Pure Appl. Chem.* **2001**, *73*, 639−665. (c) Raymo, F. M.; Tomasulo, M. Electron and Energy Transfer Modulation with Photochromic Switches. *Chem. Soc. Rev.* **2005**, *34*, 327−336. (d) Yildiz, I.; Deniz, E.; Raymo, F. M. Fluorescence Modulation with Photochromic Switches in Nanostructured Constructs. *Chem. Soc. Rev.* **2009**, *38*, 1859−1867. (e) Lebeaua, B.; Innocenzi, P. Hybrid Materials for Optics and Photonics. *Chem. Soc. Rev.* **2011**, *40*, 886−906.

(3) (a) Matsuda, K.; Irie, M. A Diarylethene with Two Nitronyl Nitroxides: Photoswitching of Intramolecular Magnetic Interaction. *J. Am. Chem. Soc.* **2000**, *122*, 7195−7201. (b) Aldoshin, S. M. Heading to Photoswitchable Magnets. *J. Photochem. Photobiol. A* **2008**, *200*, 19−33.

(4) (a) Matsuda, K.; Irie, M. Effective Photoswitching of Intramolecular Magnetic Interaction by Diarylethene: Backgrounds and Applications. *Polyhedron* **2005**, *24*, 2477−2483. (b) Tanifuji, N.; Matsuda, K.; Irie, M. Synthesis of a New Diarylethene Diradical Which Has Extended π-Conjugated Chains from the 2,5-Position of One Thiophene Ring. *Polyhedron* **2005**, *24*, 2484−2490. (c) Matsuda, K. Photoswitching of Intramolecular Magnetic Interaction Using Diarylethene Photochromic Spin Couplers. *Bull. Chem. Soc. Jpn.* **2005**, *78*, 383−392. (d) Tanifuji, N.; Irie, M.; Matsuda, K. New Photoswitching Unit for Magnetic Interaction: Diarylethene with 2,5-Bis(arylethynyl)-3-thienyl Group. *J. Am. Chem. Soc.* **2005**, *127*, 13344−13353. (e) Tanifuji, N.; Matsuda, K. M.; Irie, M. Effect of Imino Nitroxyl and Nitronyl Nitroxyl Groups on the Photochromic Reactivity of Diarylethenes. *Org. Lett.* **2005**, *7*, 3777−3780. (f) Matsuda, K.; Irie, M. Diarylethene as a Photoswitching Unit. *J. Photochem. Photobiol., C* **2004**, *5*, 169−182. (g) Matsuda, K.; Matsuo, M.; Irie, M. Photoswitching of Intramolecular Magnetic Interaction Using Diarylethene with Oligothiophene π-Conjugated Chain. *J. Org. Chem.* **2001**, *66*, 8799−8803.

(5) Ciofini, I.; Lainé, P. P.; Zamboni, M.; Daul, C. A.; Marvaud, V.; Adamo, C. Intramolecular Spin Alignment in Photomagnetic Molecular Devices: A Theoretical Study. *Chem.—Eur. J.* **2007**, *13*, 5360−5377.

(6) (a) Ali, Md. E.; Datta, S. N. Density Functional Theory Prediction of Enhanced Photomagnetic Properties of Nitronyl Nitroxide and Imino Nitroxide Diradicals with Substituded Dihydropyrene Couplers. *J. Phys. Chem. A* **2006**, *110*, 10525−10527. (b) Bhattacharjee, U.; Panda, A.; Latif, I. A.; Datta, S. N. Unusually Large Coupling Constants in Diradicals Obtained from Excitation of Mixed Radical Centers: A Theoretical Study on Potential Photomagnets. *J. Phys. Chem. A* **2010**, *114*, 6701−6704. (c) Saha, A.; Latif, I. A.; Datta, S. N. Photoswitching Magnetic Crossover in Organic Molecular Systems. *J. Phys. Chem. A* **2011**, *115*, 1371−1379.

(7) Shil, S.; Misra, A. Photoinduced Antiferromagnetic to Ferromagnetic Crossover in Organic Systems. *J. Phys. Chem. A* **2010**, *114*, 2022−2027.

(8) Boggio-Pasqua, M.; Bearpark, M. J.; Robb, M. A. Toward a Mechanistic Understanding of the Photochromism of Dimethyldihydropyrenes. *J. Org. Chem.* **2007**, *72*, 4497−4503.

(9) Matsumoto, I.; Ciofini, I.; Lainé, P. P.; Teki, Y. Intramolecular Spin Alignment within Mono-oxidized and Photoexcited Anthracene-Based π-Radicals as Prototypical Photomagnetic Molecular Devices: Relationships Between Electrochemical, Photophysical, and Photochemical Control Pathways. *Chem.—Eur. J.* **2009**, *15*, 11210−11220.

(10) (a) Dietz, F.; Olbrich, G.; Karabunarliev, S.; Tyutyulkov, N. Photoswitching of Dipole Moments, Charge-Transfer and Spectroscopic Properties. *Chem. Phys. Lett.* **2003**, *379*, 11−19. (b) Mitchell, R. H.; Bandyopadhyay, S. Linked Photoswitches Where Both Photochromes Open and Close. *Org. Lett.* **2004**, *6*, 1729−1732. (c) Drebova, N.; Tyutyulkova, N.; Karabunarlievb, S.; Dietz, F. Photoswitching of Redox Potentials and Spectroscopic Properties in the UV/Vis Region. *Z. Naturforsch. B* **2005**, *60*, 75−82. (d) Mitchell, R. H.; Bohne, C.; Wang, Y.; Bandyopadhyay, S.; Wozniak, C. B. Multistate π Switches: Synthesis and Photochemistry of a Molecule Containing Three Switchable Annelated Dihydropyrene Units. *J. Org. Chem.* **2006**, *71*, 327−336. (e) Andrasson, J.; Straight, S. D.; Bandyopadhyay, S.; Mitchell, R. H.; Moore, T. A.; Moore, A. L.; Gust, D. Molecular 2:1 Digital Multiplexer. *Angew. Chem., Int. Ed.* **2007**, *46*, 958−961. (f) Lin, Y.; Lai, Y. H. Effect of Higher Nonbenzenoids in Optical Properties of Dihydropyrene−Thiophene and Dihydropyrene−Phenylenevinylene Copolymers. *J. Polym. Sci., Part A: Polym. Chem.* **2009**, *47*, 1795−1803.

(11) Ayub, K.; Robinson, S. G.; Twamley, B.; Williams, R. V.; Mitchell, R. H. Suppressing the Thermal Metacyclophanediene to Dihydropyrene Isomerization: Synthesis and Rearrangement of 8,16-Dicyano[2.2]-metacyclophane-1,9-diene and Evidence Supporting the Proposed Biradicaloid Mechanism. *J. Org. Chem.* **2008**, *73*, 451−456.

(12) Williams, R. V.; Edwards, W. D.; Mitchell, R. H.; Robinson, S. G. A DFT Study of the Thermal, Orbital Symmetry Forbidden, Cyclophanediene to Dihydropyrene Electrocyclic Reaction. Predictions To Improve the Dimethyldihydropyrene Photoswitches. *J. Am. Chem. Soc.* **2005**, *127*, 16207−16214.

(13) (a) Blattmann, H. A; Schmidt, W. Über Die Phototropie Des Trans-15,16-Dimethyldihydropyrens und Seiner Derivate. *Tetrahedron* **1970**, *26*, 5885−5899. (b) Mitchell, R. H. The Metacyclophanediene-Dihydropyrene Photochromic π Switch. *Eur. J. Org. Chem.* **1999**, *11*, 2695−2703.

(14) (a) Koivisto, B. D.; Hick, R. G. The Magnetochemistry of Verdazyl Radical-based Materials. *Coord. Chem. Rev.* **2005**, *249*, 2612−2630. (b) Gilroy, J. B.; McKinnon, S. D. J.; Kennepohl, P.; Zsombor, M. S.; et al. Probing Electronic Communication in Stable Benzene-Bridged Verdazyl Diradicals. *J. Org. Chem.* **2007**, *72*, 8062−8069. (c) Brook, D. J. R.; Yee, G. T.; Hundley, M.; Rogow, D.; Wong, J.; Van-Tu, K. Geometric Control of Ground State Multiplicity in a Copper(I) Bis(verdazyl) Complex. *Inorg. Chem.* **2010**, *49*, 8573−8577.

(15) (a) Neugebauer, F. A.; Fischer, H. 6-Oxoverdazyls. *Angew. Chem., Int. Ed. Engl.* **1980**, *19*, 724−725. (b) Plater, M. J.; Kemp, S.; Coronado, E.; Gomez-Garcia, C. J.; Harrington, R. W.; Clegg, W. A Stable Oxoverdazyl Free Radical: Structural and Magnetic Characterization. *Polyhedron* **2006**, *25*, 2433−2438.

(16) (a) Trindle, C.; Datta, S. N. Molecular Orbital Studies on the Spin States of Nitroxide Species: Bis- and Tris-nitroxymetaphenylene, 1,1-Bisnitroxyphenylethylene, and 4,6-Dimethoxy-1,3-dialkylnitroxybenzenes. *Int. J. Quantum Chem.* **1996**, *57*, 781−799. (b) Trindle, C.; Datta, S. N.; Mallik, B. Phenylene Coupling of Methylene Sites. The Spin States of Bis(X-methylene)-*p*-phenylenes and Bis-(chloromethylene)-*m*-phenylene. *J. Am. Chem. Soc.* **1997**, *119*, 12947−12951.

(17) (a) Borden, W. T.; Davidson, E. R. Effects of Electron Repulsion in Conjugated Hydrocarbon Diradicals. *J. Am. Chem. Soc.* **1977**, *99*, 4587−4594. (b) Borden, W. T.; Davidson, E. R.; Feller, D. RHF and Two-Configuration SCF Calculations are Inappropriate for Conjugated Diradicals. *Tetrahedron* **1982**, *38*, 737−739. (c) Feller, D.; Davidson, E. R.; Borden, W. T. Ab Initio Calculations of the Energy Difference between Trimethylenemethane and Butadiene. *Isr. J. Chem.* **1983**, *23*, 105−108. (d) Kato, S.; Morokuma, K.; Feller, D.; Davidson, E. R.; Borden, W. T. Ab Initio Study of *m*-Benzoquinodimethane. *J. Am. Chem. Soc.* **1983**, *105*, 1791−1795.

(18) (a) Noodleman, L. Valence Bond Description of Antiferromagnetic Coupling in Transition Metal Dimers. *J. Chem. Phys.* **1981**, *74*, 5737−5744. (b) Noodleman, L.; Baerends, E. J. Electronic Structure, Magnetic Properties, ESR, and Optical Spectra for 2-Iron Ferredoxin Models by LCAO-Xα Valence Bond Theory. *J. Am. Chem. Soc.* **1984**, *106*, 2316−2327. (c) Noodleman, L.; Davidson, E. R. Ligand Spin Polarization and Antiferromagnetic Coupling in Transition Metal Dimers. *Chem. Phys.* **1986**, *109*, 131−143. (d) Noodleman, L.; Peng, C. Y.; Case, D. A.; Mouesca, J. M. Orbital Interactions, Electron Delocalization and Spin Coupling in Iron−Sulfur Clusters. *Coord. Chem. Rev.* **1995**, *144*, 199−244.

(19) (a) Yamaguchi, K.; Takahara, Y.; Fueno, T.; Nasu, K. Ab Initio MO Calculations of Effective Exchange Integrals between Transition-Metal Ions via Oxygen Dianions: Nature of the Copper−Oxygen Bonds and Superconductivity. *Jpn. J. Appl. Phys.* **1987**, *26*, L1362−L1364. (b) Yamaguchi, K.; Jensen, F.; Dorigo, A.; Houk, K. N. A Spin Correction Procedure for Unrestricted Hartree-Fock and Møller−Plesset Wavefunctions for Singlet Diradicals and Polyradicals. *Chem. Phys. Lett.* **1988**, *149*, 537−542. (c) Yamaguchi, K.; Takahara, Y.; Fueno, T.; Houk, K. N. Extended Hartree−Fock (EHF) Theory of Chemical Reactions. *Theor. Chim. Acta* **1988**, *73*, 337−364.

(20) (a) Becke, A. D. Density-functional thermochemistry. III. The role of exact exchange. *J. Chem. Phys.* **1993**, *98*, 5648−5652. (b) Lee, C.; Yang, W.; Parr, R. G. Development of the Colle−Salvetti Correlation-Energy Formula into a Functional of the Electron Density. *Phys. Rev. B* **1988**, *37*, 785−789.

(21) (a) Frisch, M. J.; Trucks, G. W.; et al. *Gaussian 03, Revision C.02*; Gaussian, Inc.: Wallingford, CT, 2004. (b) Frisch, M. J.; Trucks, G. W.; et al. *Gaussian 09, Revision A.1*; Gaussian, Inc.: Wallingford, CT, 2009.

(22) Kitagawa, Y.; Saito, T.; Nakanishi, Y.; Kataoka, Y.; Matsui, T.; Kawakami, T.; Okumura, M.; Yamaguchi, K. Development of

Approximately Spin Projected Energy Derivatives for Biradical Systems. *Int. J. Quantum Chem.* **2010**, *110*, 3053−3060.
(23) (a) Novoa, J. J.; Deumal, M.; Jornet-Somoza, J. Calculation of Microscopic Exchange Interactions and Modeling of Macroscopic Magnetic Properties in Molecule-Based Magnets. *Chem. Soc. Rev.* **2011**, *40*, 3182−3212. (b) Moreira, I. P. R.; Illas, F. A Unified View of the Theoretical Description of Magnetic Coupling in Molecular Chemistry and Solid State Physics. *Phys. Chem. Chem. Phys.* **2006**, *8*, 1645−1659. (c) Ciofini, I.; Daul, C. A. DFT Calculations of Molecular Magnetic Properties of Coordination Compounds. *Coord. Chem. Rev.* **2003**, *238*−*239*, 187−209.
(24) (a) Runge, E.; Gross, E. K. U. Density-Functional Theory for Time-Dependent Systems. *Phys. Rev. Lett.* **1984**, *52*, 997−1000. (b) Van Leeuwen, R. Causality and Symmetry in Time-Dependent Density-Functional Theory. *Phys. Rev. Lett.* **1998**, *80*, 1280−1283.
(25) Zhao, Y.; Truhlar, D. G. The M06 Suite of Density Functionals for Main Group Thermochemistry, Thermochemical Kinetics, Noncovalent Interactions, Excited States, and Transition Elements: Two New Functionals and Systematic Testing of Four M06-Class Functionals and 12 Other Functionals. *Theor. Chem. Acc.* **2008**, *120*, 215−241.
(26) Ko, K. C.; Cho, D.; Lee, J. Y. Systematic Approach To Design Organic Magnetic Molecules: Strongly Coupled Diradicals with Ethylene Coupler. *J. Phys. Chem. A* **2012**, *116*, 6837−6844.
(27) Pal, A. K.; Hansda, S.; Datta, S. N.; Illas, F. Theoretical Investigation of Stilbene as Photochromic Spin Coupler. *J. Phys. Chem. A* **2013**, *117*, 1773−1783.
(28) Bleany, B.; Bowers, K. D. Anomalous Paramagnetism of Copper Acetate. *Proc. R. Soc. London, Ser. A* **1952**, *214*, 451−465.